Optical wave breaking and pulse compression due to cross-phase modulation in optical fibers

Govind P. Agrawal

AT&T Bell Laboratories, Murray Hill, New Jersey 07974

P. L. Baldeck and R. R. Alfano

Department of Electrical Engineering, The City College of the City University of New York, New York, New York 10031

Received June 27, 1988; accepted October 25, 1988

When a probe pulse copropagates with a pump pulse inside an optical fiber, the two can interact through cross-phase modulation. It is shown that an interplay between the effects of group-velocity dispersion and cross-phase modulation can lead to optical wave breaking that manifests as rapid oscillations near the leading or the trailing side of the probe pulse. Qualitative features of this new kind of optical wave breaking are discussed, as well as the conditions under which it can be observed experimentally. The probe pulse can be compressed significantly by optimizing the initial delay between the pump and probe pulses even when the two pulses experience normal dispersion in the fiber.

When an ultrashort light pulse propagates through an optical fiber, its shape and spectrum change considerably as a result of the combined effects of group-velocity dispersion (GVD) and self-phase modulation (SPM). In the normal-dispersion regime of the fiber ($\lambda \lesssim 1.3\ \mu$m), the pulse can develop rapid oscillations in the wings together with spectral side lobes as a result of a phenomenon known as optical wave breaking.[1] In this Letter we show that a similar phenomenon can lead to rapid oscillations near one edge of a weak probe pulse that copropagates with a strong pump pulse. In this case the origin of optical wave breaking is related to the combined effects of GVD and cross-phase modulation[2–10] (XPM). The basic mechanism is the same in both cases. Different parts of the pulse propagate at different speeds because of the frequency chirp imposed on the pulse by SPM or XPM. If two parts with different instantaneous frequencies overlap temporally, interference between them creates an oscillatory structure in the pulse shape. Despite the identical nature of the underlying physical mechanism, optical wave breaking can exhibit qualitatively different features because of differences in the frequency chirp induced by SPM and XPM. We discuss these differences and the conditions under which XPM-induced optical wave breaking may be observable experimentally.

Let us consider two optical pulses having nonoverlapping frequency spectra centered at wavelengths λ_1 and λ_2. After considering the frequency dependence and the intensity dependence of the modal refractive index and making the slowly varying envelope approximation, we find that the complex amplitudes A_1 and A_2 of the pulse envelopes satisfy[11]

$$\frac{\partial A_j}{\partial z} + \frac{1}{v_{gj}}\frac{\partial A_j}{\partial t} + \frac{i}{2}\beta_j\frac{\partial^2 A_j}{\partial t^2} + \frac{\alpha_j}{2}A_j = i\gamma_j(|A_j|^2 + 2|A_{3-j}|^2)A_j, \quad (1)$$

where $j = 1$ or 2, v_{gj} is the group velocity, β_j is the GVD coefficient, and α_j is the attenuation coefficient. The nonlinearity parameter γ_j is related to the nonlinear-index coefficient n_2 by the equation

$$\gamma_j = \frac{2\pi n_2}{\lambda_j A_{\text{eff}}}, \quad (2)$$

where A_{eff} is the effective core area. A four-wave mixing term has been neglected in Eq. (1) after assuming that phase matching does not occur. The last term in Eq. (1) is due to XPM and is responsible for the mutual coupling between the two pulses. It is this XPM-induced coupling that gives rise to the optical wave breaking discussed below.

It is useful to introduce the normalized variables by using the definitions

$$\xi = \frac{z}{L_D}, \qquad \tau = \frac{(t - z/v_{g1})}{T_0}, \qquad U_j = \frac{A_j}{\sqrt{P_1}} \quad (3)$$

and to write the coupled amplitude equations from Eq. (1) in the form of

$$\frac{\partial U_1}{\partial \xi} + \frac{i}{2}\,\text{sgn}(\beta_1)\frac{\partial^2 U_1}{\partial \tau^2} = iN^2(|U_1|^2 + 2|U_2|^2)U_1, \quad (4)$$

$$\frac{\partial U_2}{\partial \xi} \pm \frac{L_D}{L_W}\frac{\partial U_2}{\partial \tau} + \frac{i}{2}\frac{\beta_2}{|\beta_1|}\frac{\partial^2 U_2}{\partial \tau^2} = iN^2\frac{\lambda_1}{\lambda_2}(|U_2|^2 + 2|U_1|^2)U_2, \quad (5)$$

where

$$L_D = \frac{T_0^2}{|\beta_1|}, \qquad L_W = \frac{v_{g1}v_{g2}T_0}{|v_{g1} - v_{g2}|}, \quad (6)$$

and

0146-9592/89/020137-03$2.00/0

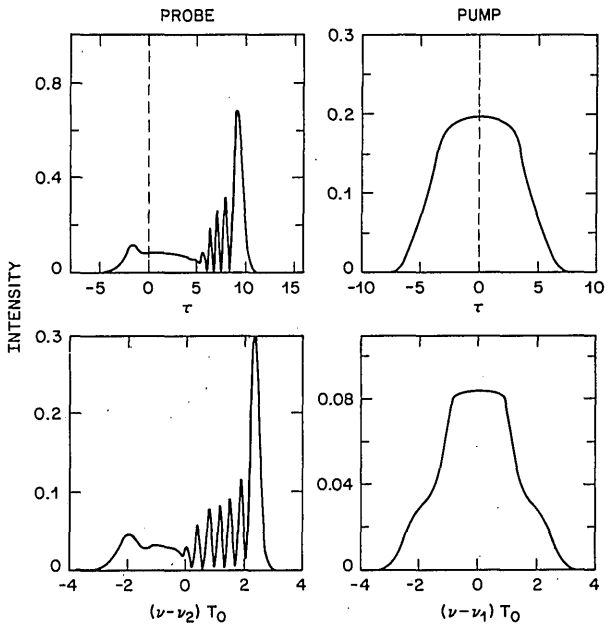

Fig. 1. Shape and spectrum of the probe pulse (left-hand side) and the pump pulse (right-hand side) at $z/L_D = 0.4$ when the two pulses copropagate in the normal-dispersion regime of a single-mode fiber. The parameters are $N = 10$, $L_W/L_D = 0.1$, $\lambda_1/\lambda_2 = 1.2$, and $\tau_d = 0$. Oscillations near the trailing edge ($\tau > 0$) of the probe pulse are due to XPM-induced optical wave breaking.

$$N^2 = \gamma_1 P_1 L_D = \gamma_1 P_1 T_0^2/|\beta_1|. \tag{7}$$

Here T_0 is the pulse width and P_1 is the peak power of pulse 1. The dispersion length L_D provides a length scale over which the GVD effects become important. The walk-off length L_W is another length scale resulting from the group-velocity mismatch. Since the two pulses generally travel at different speeds, they separate from each other over a distance of a few walk-off lengths and cease to interact through XPM. The choice of sign in Eq. (5) depends on the sign of $v_{g1} - v_{g2}$; the positive sign corresponds to $v_{g1} > v_{g2}$. The parameter N measures the relative importance of the nonlinear effects. Although N has physical significance only in the anomalous-dispersion regime of the fiber, where its integer values correspond to fundamental and higher-order solitons, it is a useful dimensionless parameter in the case of normal dispersion. For simplicity, we have neglected the loss term in Eqs. (4) and (5). This is not a limitation since the fiber loss is generally negligible for fiber lengths commonly used in the XPM experiments.

To isolate the effects of XPM from those of SPM, a pump–probe configuration is generally used in the experiments.[4,6] We assume that $|U_2|^2 \ll |U_1|^2$ so that pulse 1 plays the role of the pump pulse and propagates without being affected by the copropagating probe pulse. The probe pulse, however, interacts with the pump pulse through XPM. To study how XPM affects the probe evolution along the fiber, we have solved Eqs. (4) and (5) numerically using a generalization of the beam-propagation or the split-step Fourier method.[11] The numerical results depend strongly on the relative magnitudes of the length scales L_D and L_W. If $L_W \ll L_D$, the pulses walk off from each other before GVD has an opportunity to influence the pulse evolution. However, if L_W and L_D become comparable ($L_W/L_D \gtrsim 0.1$), both XPM and GVD can act together and modify the pulse shape and spectrum with new features. To show these features, we consider a specific case in which $L_W/L_D = 0.1$ and $\lambda_1/\lambda_2 = 1.2$. Both pulses are assumed to propagate in the normal GVD regime with $\beta_1 \simeq \beta_2 > 0$. The positive sign is chosen in Eq. (5) to ensure that the pump pulse travels faster than the probe pulse ($v_{g1} > v_{g2}$). At the fiber input both pulses are taken to be a Gaussian of the same width T_0 (FWHM $\simeq 1.66T_0$), i.e.,

$$U_1(0, \tau) = \exp(-\tau^2/2),$$
$$U_2(0, \tau) = (P_2/P_1)\exp[-(\tau - \tau_d)^2/2], \tag{8}$$

where τ_d accounts for an initial delay between the two pulses. The peak-power ratio $P_2/P_1 = 10^{-4}$ in order to simulate a pump–probe configuration.

Consider first the case $\tau_d = 0$ so that the two pulses overlap completely at $z = 0$. Figure 1 shows the shapes and spectra of the pump and probe pulses at $\xi = 0.4$ obtained by solving Eqs. (4) and (5) numerically with $N = 10$. It is evident that GVD can substantially affect the evolution features expected from SPM or XPM alone. The XPM effects are absent for the pump pulse. The pump shape and the spectrum shown on the right-hand side exhibit features expected from dispersive SPM for $N = 10$. The left-hand side shows the shape and the spectrum of the probe pulse whose evolution is governed by dispersive XPM. In the absence of GVD, the probe shape would be a narrow Gaussian centered at $\tau = 4$ (the relative delay at the fiber output because of group-velocity mismatch). The GVD effects not only broaden the pulse considerably but also induce rapid oscillations near the trailing edge of the probe pulse. These oscillations are due to XPM-induced optical wave breaking.

To understand the origin of XPM-induced optical wave breaking, it is useful to consider the frequency

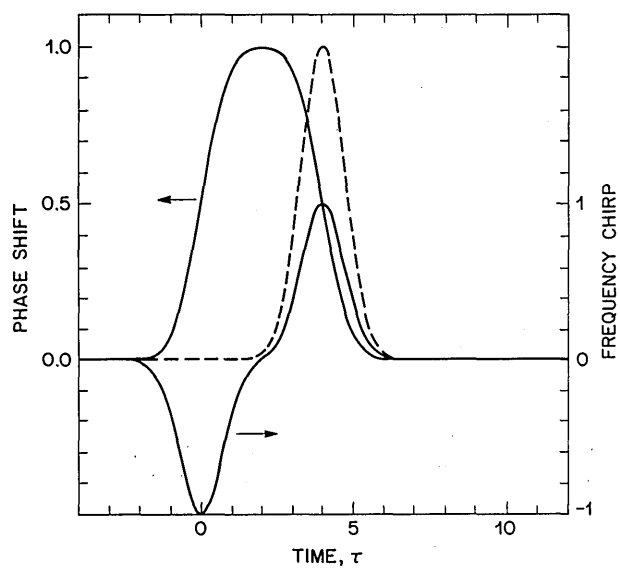

Fig. 2. XPM-induced phase shift and frequency chirp for the probe pulse whose shape is shown by the dashed curve.

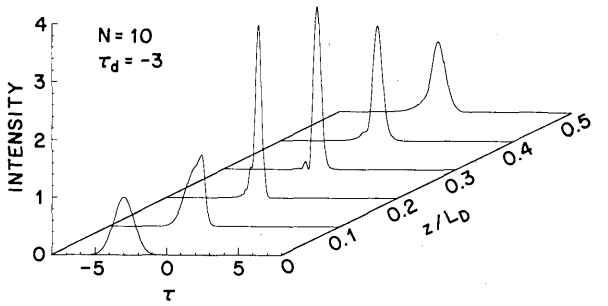

Fig. 3. Evolution of the probe pulse for $\tau_d = -3$. The other parameters are identical to those of Fig. 1.

chirp imposed on the probe pulse by the copropagating pump pulse. In the absence of GVD, we can use the phase-shift model of Ref. 6. For the case of a Gaussian pulse, the XPM-induced phase shift of the probe pulse can be expressed in terms of an error function.[10] The result can be used to obtain the XPM-induced frequency chirp given by

$$\Delta\nu = \Delta\nu_{\max}\{\exp[-(\tau + \tau_d - z/L_W)^2] - \exp[-(\tau + \tau_d)^2]\}, \quad (9)$$

where

$$\Delta\nu_{\max} = \gamma_2 P_1 L_W/(\pi T_0). \quad (10)$$

Figure 2 shows the phase shift and the chirp $\Delta\nu/\Delta\nu_{\max}$ as a function of time for $\tau_d = 0$ and $z/L_W = 4$, the values used in Fig. 1. The location of the probe pulse is shown by the dashed curve; the pump pulse is located at $\tau = 0$. The maximum chirp occurs at the center of the probe pulse. Since the chirp is positive, the blue-shifted components are generated by XPM near the pulse center. As a result of the normal GVD, the peak of the probe pulse moves slower than its tails. Since the peak lags behind as the probe pulse propagates, it interferes with the trailing edge. Oscillations seen near the trailing edge of the probe pulse in Fig. 1 result from such an interference. Since the basic mechanism is analogous to the optical-wave-breaking phenomenon occurring in the case of dispersive SPM, we call it XPM-induced optical wave breaking.

In spite of the identical nature of the underlying physical mechanism, optical wave breaking exhibits different qualitative features in the XPM case compared with the SPM case. The most striking difference is that the pulse shape is asymmetric, with only one edge developing oscillations. For the case shown in Fig. 1, oscillations occur near the trailing edge because the faster-moving pump pulse interacts mainly with the trailing edge. If the probe and pump wavelengths were reversed so that the pump pulse moved slower than the probe pulse, oscillations would occur near the leading edge since the pump pulse would interact mainly with that edge.

We discuss briefly the effect of initial relative time delay between the two pulses on optical wave breaking. Figure 3 shows probe evolution for $\tau_d = -3$, i.e., the probe is advanced by $3T_0$ with respect to the faster-moving pump pulse. The other parameters are identical to those of Fig. 1, where $\tau_d = 0$. In contrast with the $\tau_d = 0$ case, where GVD led to a large broadening of the probe, the probe pulse goes through an initial stage of compression. We have carried out numerical simulations over large ranges of τ_d and N to quantify the extent of XPM-induced pulse compression. For $N = 10$, the probe pulse can be compressed by a factor of ~3–6 when $|\tau_d|$ is in the range of 1–4. The compression factor can be increased by increasing the pump power or the parameter N. The optimum fiber length for maximum compression is well approximated by $z_{\text{opt}} \simeq |\tau_d| L_W$. The physical mechanism behind pulse compression is the pump-induced frequency chirp given by Eq. (9). For $\tau_d = -3$, the chirp is nearly linear and negative (frequency decreases with time) over the trailing part of the probe pulse. The normal GVD compresses the trailing part, as seen clearly in Fig. 3. This compression technique is different from that of Ref. 12, where an external grating pair is needed. It is analogous to the soliton-effect compression technique except that XPM-induced compression can occur even in the normal-GVD regime of the fiber.

The experimental observation of XPM-induced optical wave breaking would require the use of femtosecond pulses. This can be seen by noting that for picosecond pulses with $T_0 = 5$–10 psec, typically $L_D \sim 1$ km while $L_W \sim 1$ m, even if the pump–probe wavelengths differ by as little as 10 mm. By contrast, if $T_0 = 100$ fsec, L_D and L_W become comparable (~10 cm) and the temporal changes in the probe shape discussed here can occur in a fiber less than a meter long. Pulses much shorter than 100 fsec should also not be used since the higher-order nonlinear effects such as self-steepening and a delayed nonlinear response then become increasingly more important. Finally, XPM may be useful for compressing weak femtosecond pulses by launching them together with the intense pump pulses and by optimizing the initial delay between the two.

The research at The City College of New York is partially supported by Hamamatsu Photonics K.K.

References

1. W. J. Tomlinson, R. H. Stolen, and A. M. Johnson, Opt. Lett. **10,** 457 (1985).
2. J. I. Gersten, R. R. Alfano, and M. Belic, Phys. Rev. A **21,** 1222 (1980).
3. A. A. Chraplyvy and J. Stone, Electron. Lett. **20,** 996 (1984).
4. R. R. Alfano, Q. X. Li, T. Jimbo, J. T. Manassah, and P. P. Ho, Opt. Lett. **11,** 628 (1986).
5. D. Schadt, B. Jaskorzynska, and U. Osterberg, J. Opt. Soc. Am. B **3,** 1257 (1986).
6. M. N. Islam, L. F. Mollenauer, R. H. Stolen, J. R. Simpson, and H. T. Shang, Opt. Lett. **12,** 625 (1987).
7. G. P. Agrawal, Phys. Rev. Lett. **59,** 880 (1987).
8. R. R. Alfano, P. L. Baldeck, F. Raccah, and P. P. Ho, Appl. Opt. **26,** 3491 (1987).
9. D. Schadt and B. Jaskorzynska, Electron. Lett. **23,** 1090 (1987).
10. P. L. Baldeck, R. R. Alfano, and G. P. Agrawal, Appl. Phys. Lett. **52,** 1939 (1988).
11. G. P. Agrawal, *Nonlinear Fiber Optics* (Academic, Boston, Mass., 1989), Chap. 2.
12. J. T. Manassah, Opt. Lett. **13,** 755 (1988).